Contents lists available at ScienceDirect

Composite Structures

On the temperatures developed in CFRP drilling using uncoated WC-Co tools Part I: Workpiece constituents, cutting speed and heat dissipation

J.L. Merino-Pérez [a,*], R. Royer [b], S. Ayvar-Soberanis [c], E. Merson [b], A. Hodzic [d]

[a] Industrial Doctorate Centre in Machining Science, Department of Mechanical Engineering, The University of Sheffield, Sir Frederick Mappin Building, Mappin Street, Sheffield S1 3JD, UK
[b] Sandvik Coromant, Sandvik AB, Advanced Manufacturing Park, Unit 8, Morse Way, Waverley, Sheffield S60 5BJ, UK
[c] Advanced Manufacturing Research Centre with Boeing, The University of Sheffield, Advanced Manufacturing Park, Wallis Way, Catcliffe, Rotherham S60 5TZ, UK
[d] Composite Systems Innovation Centre, Department of Mechanical Engineering, The University of Sheffield, Sir Frederick Mappin Building, Mappin Street, Sheffield S1 3JD, UK

ARTICLE INFO

ABSTRACT

This work investigated the influence of the material properties and cutting speed on the heat dissipation in the drilling of carbon fibre reinforced plastic (CFRP) composites using uncoated WC-Co tools. The first stage of the investigation compared the heat dissipation in drilling three different CFRP systems by measuring the temperatures developed at different distances around the borehole using thermocouples and an infra-red camera. The second stage studied the influence of cutting speed on the maximum temperatures developed in the workpiece in drilling a selected CFRP system in a cutting speed range from 50 to 200 m/min. The cross-linking density of the polymer matrix and the degree of crystallinity and structure of the carbon fibres exhibited a significant influence on the overall temperature and on the heat dissipation, whereas 150–200 m/min cutting speeds yielded higher concentration of heat, compared to 50–100 m/min cutting speeds.

1. Introduction

The study of temperatures developed in the machining process of fibre reinforced plastics (FRP) composites has been of interest since FRPs became extensively used in the aerospace and automotive industries. A number of temperature acquisition methods used to measure and monitor different machining operations, comprising and combining experimental, numerical and analytical techniques, were studied and reported in the literature. The use of thermocouples embedded in the tool was the earliest and most common method used to measure the temperatures and the thermal gradients that occurred on the cutting edges of the selected tools during the machining process. In this method, thermocouples are embedded in the tool by machining adequate grooves and applying highly thermally conductive adhesives. Using small diameter thermocouples allows the temperatures developed along the cutting edge to be mapped. However, it is not possible to place thermocouples at the cutting edge, where the highest temperatures develop during the process [1,2]. Embedding thermocouples

in the rotating part of the system added complexity to the challenge of transmitting and recording the data.

Earlier studies set the tool as the static part of the drilling set-up and modified the workpiece to be attached to the spindle [3,4], however this arrangement allowed only one hole to be drilled at a time, making it difficult to reach a steady state temperature.

Another solution utilised wireless systems to transmit the data from the spindle in the machining of metals, alloys and CFRP composites [5,6]. The transmission system consisted of a special tool holder, which is formed by a radio frequency (RF) transmitter and an antenna. This system featured a high acquisition frequency (1 kHz) and a much reduced delay (150 µs). This wireless system provided good results, however considering that each tool requires individual preparation for its use in the RF system, the cost of the wireless tool holder makes this choice an expensive solution.

Other studies reported the choice of the dynamic thermocouple as an alternative method [1,2,7–9]. This technique utilises the tool and the workpiece forming a dynamic thermocouple, and requires previous characterisation and calibration of the system to relate the electromotive force to the developed temperatures. This method has been successfully applied in mapping the temperatures along the cutting edge in the drilling of aluminium [8] and monitoring the temperatures developed in CFRP milling [9]. However, the poor electrical conductivity of FRP composites

* Corresponding author. Tel.: +44 7592 962654.
E-mail addresses: j.merino@sheffield.ac.uk (J.L. Merino-Pérez), raphael.royer@sandvik.com (R. Royer), s.ayvar@amrc.co.uk (S. Ayvar-Soberanis), eleanor.merson@sandvik.com (E. Merson), a.hodzic@sheffield.ac.uk (A. Hodzic).

complicates the preparation and characterisation of the dynamic thermocouple. A good number of authors considered the utilisation of non-contact and infra-red radiation techniques (pyrometers-optical fibres, optical infra-red radiation) to measure the temperatures developed in a number of machining operations [1,2,7,10–12]. These methods are limited to temperature acquisition and monitoring of uncovered surfaces and require calibration before their use to determine their emissivity and reflectivity, since the measurement is very sensitive to these parameters. However, infra-red cameras represent a fast and very accurate temperature measurement method.

Reported investigations studied the influence of the cutting parameters on the tool temperature in the drilling of CFRP laminates by embedding thermocouples in the tool [4,13,14]. Authors studied the influence of cutting speed in a 35–200 m/min range and reported an increased flank surface temperature with the increasing cutting speed. However, the study of the influence of feed rate (0.05–0.4 mm/rev range) on flank surface temperature yielded the contradicting results. Chen reported a decreased flank surface temperature with the increasing feed rate [13], whereas a more recent study by Weinert and Kempmann reported the contrary [4]. The different workpiece thicknesses (2 and 17 mm) and the experimental arrangement utilised in both investigations (workpiece as the rotatory element) could have prevented the tool from reaching a steady state temperature [14], thus explaining the difference in the reported results.

Tian and Cole reported the impact of the material constituents on the physical properties of CFRP composites. Both fibre volume fraction and direction exhibited significant influence on the in-plane and through thickness thermal conductivities of CFRP composites [11].

On the other hand, Knibbs and Morris reported that small misalignment of fibres in the composite showed to have limited influence on the thermal conductivity and significant impact on Young's modulus in the directions parallel to the reinforcement. However, thermal conductivity was affected to a greater extent in the transverse direction [15].

The type of fibres also showed to have significant impact on the thermal and mechanical properties of CFRP composites. Thermal conductivity and modulus of elasticity of CFRP composites having high modulus carbon fibre reinforcement exceeded that of high strength carbon fibres, which was attributed to the higher degree of crystallinity of the high modulus reinforcement [16,17].

The work presented in this investigation utilised two widely accepted temperature acquisition methods, data collection using thermocouples and thermal imaging (infra-red camera), to assess the impact that the material properties of selected CFRP systems (having different cross-linking densities and fibres crystallinity) and the cutting speed have on the maximum developed temperatures and on the heat dissipation in the drilling of CFRP composites.

2. Materials and methods

2.1. Composite systems

The CFRP plates used in this investigation were manufactured at the Composite Centre of the Advanced Manufacturing Research Centre with Boeing, The University of Sheffield. These plates were made from woven carbon fibre (CF) and epoxy prepreg plies having 55% fibre volume fraction (V_f), supplied by Cytec Engineered Materials. Initially, 350×350 mm plates were made by vacuum bag moulding method, laying up 42 prepreg plies (0° orientation laminate) to approximate thickness of 10 mm. Following the lay-up process, the plates were cured and post-cured in an autoclave, following the specifications provided by the manufacturer to develop

their full mechanical performance and the maximum glass transition temperature (T_g). Then, the plates were cut down to a size of 310×155 mm using a WardJet G-Series 5-axis water-jet CNC machine.

Three different CFRP systems were considered in this investigation:

- MTM44-1 and CF0300,
- MTM44-1 and CF2216, and
- MTM28B and CF0300.

MTM44-1 resin is a toughened phenol–formaldehyde (PF)-based aerospace grade resin, whereas MTM28B is a toughened epoxy DGEBA-based automotive grade resin. CF0300 is a 2/2 twill carbon fabric, 3 K high strength (HS) carbon fibre reinforcement, while CF2216 is a 2/2 twill carbon fabric, 6 K high modulus (HM) carbon fibre reinforcement, both having density of 199 g/cm³.

Dynamic mechanical analysis (DMA) and thermo-mechanical analysis (TMA) techniques were utilised to measure the glass transition temperature (T_g) and coefficient of thermal expansion (CET) of MTM44-1 and MTM28B resins. The DMA device utilised to study the glass transition temperature of the selected resins was a *Metraviv VA2000 ViscoAnalyseur* using a 3-point bend configuration. The specimens were tested in a single-frequency mode (10 Hz), applying static and dynamic displacements of -80 μm and 50 μm respectively and performing temperature sweeps ranging from room temperature to 160 °C (MTM28B) and 250 °C (MTM44-1) at a 3 °C/min heating rate. Coefficients of thermal expansion were measured utilising a *Perkin Elmer Diamond TMA* applying a force of 10 mN and performing temperature sweeps ranging from 35 °C to 160 °C (MTM28B) and 250 °C (MTM44-1) at a 5 °C/min heating rate.

2.2. Drilling tool

The main tool used in this investigation was ø6.35 mm two flute double angle WC-10%Co uncoated Sandvik Coromant's CoroDrill 856 drill bit. The main geometry features of this tool are 120° and 40° point angles (chamfered geometry), 25° helix angle, 12° primary clearance angle, 20° secondary clearance angle and 0.64 mm margin width. All the drill bits used in this investigation were manufactured in the same batch, having a maximum lip height variation of 25 μm, a maximum web eccentricity of 100 μm and a chisel edge centrality of 0.05 mm. The tool utilised to prepare the plate to embed the thermocouples was ø1.25 mm uncoated tungsten carbide Sandvik Coromant's CoroDrill 840 drill bit. The CNC machine utilised was a three-axis DMG DMU 60monoBLOCK fitted with Sandvik Coromant's CoroChuck 930 hydraulic tool holder, having a total measured run-out of 12 μm. All the machining operations in this work were conducted without coolant (dry drilling).

2.3. Thermocouples

This investigation utilised Perfluoro Alkoxy Alkene (PFA)-insulated type K fine-gauge (chromel–alumel) thermocouples manufactured and supplied by Omega Engineering, having a working temperature range from -200 °C to $+1300$ °C, 1 m long, ø0.25 mm wire and ø0.49 mm bead. According to the specifications provided by the manufacturer, the utilised thermocouples feature a response time (defined as the required time for the thermocouples to acquire 63.2% of their final temperature when the bead is alternately exposed to two different temperatures) of 0.22 s, measured with exposures between 93 °C and 38 °C in still water. A Pico Technology's TC-08 Thermocouples Data Logger, featuring 8-channels and automatic cold junction compensation, and Pico Log

Recorder software transmitted and recorded the acquired signals to a laptop via USB interface.

2.4. Infra-red camera

The infra-red camera utilised in this study was a Micro-Epsilon thermoIMAGER TIM 160 having 160×120 pixels optical resolution, three measuring ranges ($-20\,°C/100\,°C$, $0\,°C/200\,°C$ and $150\,°C/900\,°C$), spectral range 7.6 to 13 µm, thermal sensitivity of 0.08 K and 120 Hz frame rate. TIM Connect software controlled the camera and helped to process the acquired data.

2.5. The impact of matrix and reinforcement on the heat dissipation in CFRP drilling

The scope of this part of the study was to assess the impact that the constituents (matrix and reinforcement) of the selected CFRP systems have on the heat dissipation in the drilling of CFRP composites. Two standalone experiments, using thermocouples and infra-red camera, recorded the temperatures developed in the drilling operation at different distances around the hole edge. This stage considered three CFRP systems with different polymer matrices and types of carbon fibres, as described in 2.1. The selected cutting conditions for both experiments were $V_c = 220$ m/min (11,000 rpm) and $f_r = 0.005$ mm/rev. This combination of cutting inputs was selected for the purpose of this stage of the study only, and is not representative of the parameters used in the industry to machine composites (especially the low feed rate). However, it guaranteed reliable temperature measurements while utilising thermocouples, considering their low response time.

2.5.1. Thermocouples

In order to measure the temperatures developed around the borehole using thermocouples, 16 through-holes were drilled on each CFRP plate, forming a 4×4 array. This number of holes assured to reach a steady state temperature and low tool wear, as reported in our previous study [18]. The temperatures were measured by embedding four thermocouples in the workpiece at different distances around the last drilled hole, in the direction of the fibres (Fig. 1), according to the orthotropic material properties of the selected CFRP composites [11].
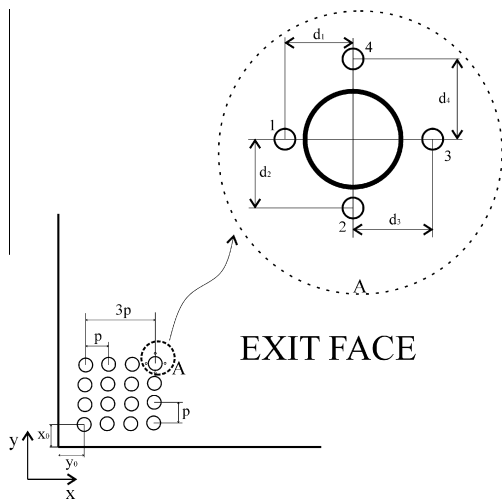
To embed the thermocouples, four 1 mm depth holes were previously drilled on the exit face of each plate using ø1.25 mm drill bit, mentioned in Section 2.2. Omega OT-201 conductive paste, having 2.31 W/(m K) thermal conductivity and 1014 Ω cm electrical insulation, was used to fill the holes and remove the air gaps (0.02–0.05 W/(m K) thermal conductivity), which allowed a better temperature acquisition. Thermocouples were fixed on the plate using adhesive tape, impeding their movement. Then, the plate was clamped on the CNC machine bed and the thermocouples were connected to the data logger, which recorded the acquired temperatures.

2.5.2. Infra-red camera

The measurement of the developed temperatures around the borehole in the drilling of CFRP composites using thermal imaging was conducted using the same number of holes and hole array as in Section 2.5.1, for a better comparison of the results. The thermal camera acquired the maximum developed temperatures at the hole exit by recording the exit face of CFRP plate. The considered CFRP composite plates were manufactured to obtain a matte surface finish on the exit face, which minimised the effect of reflectivity on the measurements. In addition to this, the exit surface of each plate was sprayed with black paint, providing a high thermal emissivity ($\varepsilon = 0.96$). Fig. 2 illustrates the experimental set-up.

To obtain reliable measurements, the image of the exit surface was manually brought into focus. The temperature window utilised during the experiment was $150\,°C/900\,°C$. After recording the data, these were processed using TIM Connect software by setting four measurement points at different distances (d_1–d_4) away from the hole edge, with the same values as explained in Section 2.5.1, for a better comparison using both methods.

2.6. Correlation between cutting speed and heat dissipation in the drilling of CFRP composites

To study the correlation between the cutting speed and the maximum temperatures developed in the drilling of CFRP composites, four selected cutting conditions were considered (Table 1). The selected CFRP system drilled in this part of the investigation was MTM44-1 CF0300, described in Section 2.1.

The experimental set-up and workpiece preparation were similar to those described in Section 2.5.2, however in this part of the study the thermal camera was placed 20 mm away from the exit surface, which increased the resolution of the captured image, and recorded the temperatures developed at the last drilled hole only. The data were processed by placing several measurement points along 2 mm length from the hole centre, as illustrated in Fig. 3.
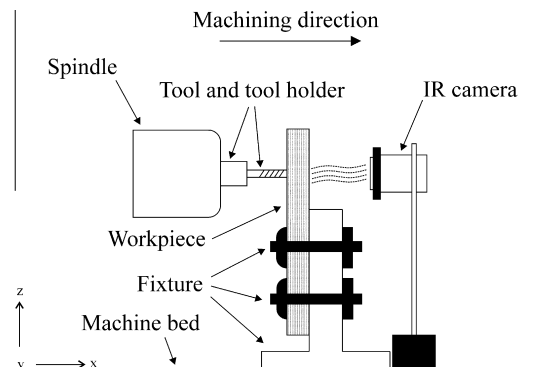

Fig. 1. View of the drilling array from the exit face. x_0 and y_0 indicate the centre of the first drilled hole. The distance between hole centres was $p = 10$ mm. The thermocouples were embedded in the workpiece by drilling four ø1.25 mm holes 1 mm depth on the exit face of the plate, around the last hole, at different distances: $d_1 = 4.175$ mm, $d_2 = 5.175$ mm, $d_3 = 6.175$ mm and $d_4 = 7.175$ mm. In this experiment, the plate was clamped flat on the machine bed.

Fig. 2. A sketch of the experimental set-up utilised to record the temperatures developed in drilling CFRP composites using the infra-red camera. Temperatures were measured at the hole exit. Fixture, workpiece and camera were fixed on the machine bed and the spindle, tool holder and tool were the moving elements.

Table 1

Selected cutting conditions to study the correlation between cutting speed and maximum temperatures developed in the drilling of CFRP composites. To achieve a steady state temperature, six consecutive holes per condition were drilled and the temperature was recorded for the last hole.

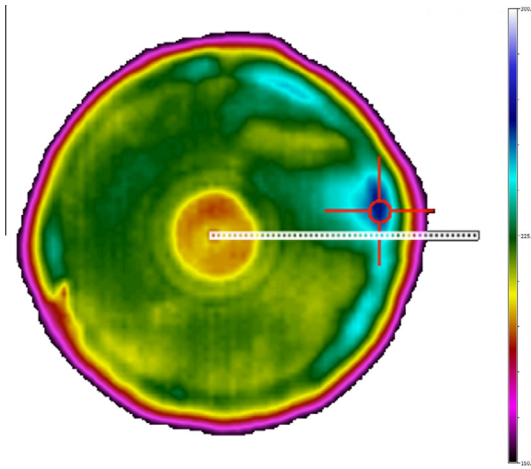|	Spindle speed [rpm]	Cutting speed [m/min]	Feed rate [mm/rev]	Feed speed [mm/min]
Condition 1	2,500	49.8	0.05	125
Condition 2	5,000	99.6		250
Condition 3	7,500	149.4		375
Condition 4	10,000	199.2		500

Fig. 3. Arrangement of the measurement points along 2 mm length from the centre of the hole. 50 points were utilised to measure the temperatures developed during the machining operation. The maximum temperature for each measurement point was recorded.

A *Carl Zeiss EVO LS25* scanning electron microscope (SEM) was utilised to inspect the surface topography of the profiles corresponding to the last drilled hole of each cutting condition. 500× and 1000× magnifications were utilised in order to capture all the surface features. This SEM features a variable pressure (VP) mode that allowed the non-conductive epoxy matrix of the selected CFRP system to be inspected without coating.

3. Results and discussion

3.1. The impact of matrix and reinforcement on the heat dissipation in CFRP drilling

Fig. 4 shows the maximum temperatures developed in four different points, recorded using thermocouples and thermal imaging. The presented results reveal a good agreement in the captured temperatures using both methods. The two studied measurement methods indicated similar trends in the thermal gradient around the borehole.

The results also showed small differences in the measurements using both methods, however these differences can be attributed to the thermocouple-workpiece thermal coupling and the low response time of the thermocouples. Even if the applied thermal paste improved the thermal conductivity between the workpiece and the thermocouples, the thermal coupling was not ideal and had an effect on the measurements. In Fig. 4(c), the developed temperature at d_4 using thermal imaging was not registered, since the temperatures developed at this point were below the lowest threshold of the selected temperature window (150 °C).

Fig. 5 illustrates the differences in the thermal gradients developed in the drilling of selected CFRP systems.
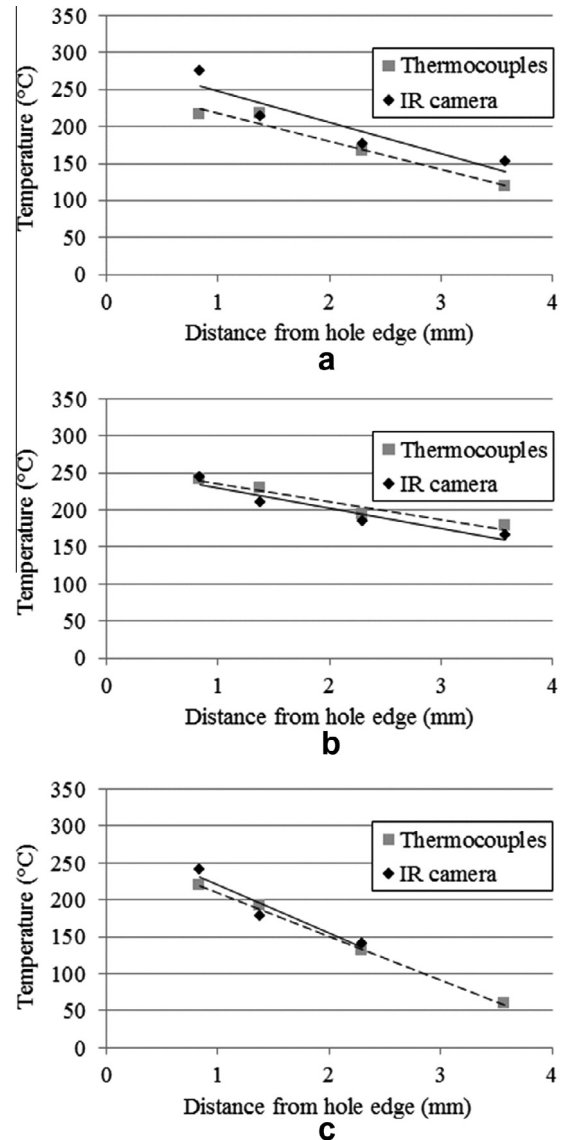

Fig. 4. Maximum temperatures developed in the drilling of selected CFRP systems: (a) MTM44-1 CF0300, (b) MTM44-1 CF2216 and (c) MTM28B CF0300 at different distances away from the hole edge, measured using thermocouples and thermal imaging (IR camera).

The selected CFRP systems developed dissimilar thermal behaviours. CFRP composites having resins with higher cross-linking density (MTM44-1) exhibited higher machining temperatures and lower thermal gradients than that having lower cross-linking density (MTM28B). Previous studies reported that the higher thermal conductivity of epoxy networks can be attributed to the densification of the network after cross-linking [19,20] and to covalent bonds formed during the cross-linking, which had the ability to transfer thermal energy more efficiently along the polymer chains, ease the heat flow and promote the phonon diffusion [21,22]. In addition to this, the literature indicated that higher cross-linking density and closer-packed polymer network enhanced the thermo mechanical properties of polymer matrices such as glass transition temperature (T_g) and elastic moduli [23–25] as well as enabling a direct correlation between thermal conductivity and elastic modulus in fibre reinforced plastic (FRP) composites [26]. Table 2 shows the glass transition temperature and coefficient of thermal expansion of the studied polymer matrices.

The higher cross-linking density and closer-packed molecular network of MTM44-1 resin compared to MTM28B resin, increased
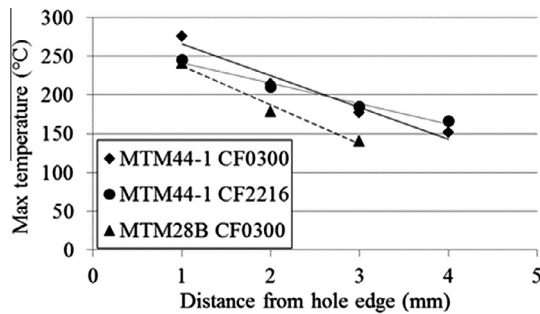
Fig. 5. Trends of the developed temperatures around the borehole in the drilling of selected CFRP systems recorded using the thermal camera.

Fig. 6. Maximum and average maximum developed temperatures in the drilling of MTM44-1 CF0300 composite at the selected cutting speeds.

Table 2
Glass transition temperature (T_g) and the coefficient of thermal expansion (CET) corresponding to MTM28B and MTM44-1 resins.

	T_g (E' onset) [°C]	T_g (tanδ) [°C]	CET (before T_g) [10^{-6}/°C]	CET (after T_g) [10^{-6}/°C]
MTM28B	104.8	136.9	~50–80	~150
MTM44-1	182.4	222.5	~60	~60

the T_g of the system and enhanced its thermal stability, as showed by the values of thermal expansion coefficient (CET) in Table 2. Below T_g, MTM28B resin exhibited CET that increased linearly with the increasing temperature and doubled its value above T_g, whereas MTM44-1 resin showed a constant CET below and above T_g, thus presenting improved thermal stability.

The drilling temperatures depicted in Figs. 4 and 5 also had a significant influence on the thermal conductivity of the composite, since in most cases these temperatures were above T_g of the polymer matrices of the selected CFRP composites (Table 2). Previous studies reported that thermal conductivity in amorphous polymers increased with the increasing temperatures below T_g, and decreased with the increasing temperatures above T_g [27], however the type of carbon fibre reinforcement showed to have more significant impact on the thermal gradients measured in the machining of the selected CFRP systems.

On the other hand, the type of reinforcement showed a significant influence on the heat dissipation in the drilling of the selected CFRP systems; however other studies reported also to have a strong influence on the maximum developed temperatures [18]. The composite having high modulus carbon fibres (CF2216) exhibited lower thermal gradient around borehole (thus higher heat dissipation) than those reinforced with high strength carbon fibres (CF0300). This can be attributed to the high degree of crystallinity of the high modulus carbon fibres [16,17]. Literature reported a significant correlation between the atomic structure, the manufacturing process and the thermo-mechanical properties of the carbon fibres. Both thermal conductivity and the degree of graphitisation increased with the increasing spinning temperature until a maximum was reached, however further increase in temperature resulted in a decrease of these properties [28]. Furthermore, ribbon-shaped carbon fibres manufactured to achieve both high crystalline graphitic structure and the degree of orientation in the direction of the fibre axis resulted in outstanding mechanical (>800 GPa Young's modulus) and thermal (>1000 W/m K) properties [29].

3.2. Correlation between cutting speed and heat dissipation in the drilling of CFRP composites

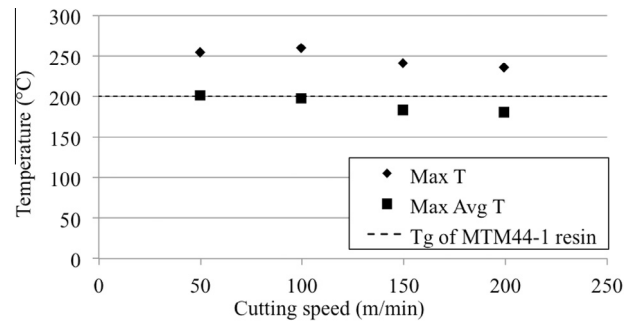Fig. 6 shows the maximum (Max T) and average maximum (Max Avg T) temperatures developed in the drilling of MTM44-1 CF0300 CFRP composite at the set cutting conditions (Table 1). Each Max T value corresponds to one of the measuring points, whereas each Max Avg T value corresponds to one of the measuring points having the highest average temperature during the cutting process (Fig. 3).

The results showed similar trends for both maximum and average maximum temperatures, where the temperature decreased with the increasing cutting speed. Cutting time is a factor that can help to explain this trend. Higher cutting speeds yielded lower cutting times; therefore the tool generated heat during a shorter time period. 50–100 m/min and 150–200 m/min cutting speed sets yielded similar maximum and maximum average temperatures, however a drop in the measured temperatures from 100 m/min to 150 m/min cutting speeds was observed. 150–200 m/min cutting speeds developed maximum average temperatures that were slightly below the glass transition temperature of the polymer matrix of the selected composite (Table 2). Below T_g, the values of storage and loss moduli were significantly higher and lower respectively than at T_g, therefore at these developed maximum average temperatures the material had the ability to store the energy from the cutting process [30,31]. These results are in disagreement with the results reported in the literature [4,13] that indicated a direct correlation between cutting speed and developed temperatures. However, the experimental arrangement utilised in these studies (workpiece as the rotatory element), could have prevented the system from reaching a steady state temperature, as it was reported in other studies [14,18]. Moreover, those studies assessed the temperatures in the tool instead of the workpiece; therefore a dissimilar tool-chip-workpiece heat partition at different cutting conditions can explain the observed difference in the reported results.

Fig. 7 shows the maximum temperature profiles developed in the drilling of the studied CFRP laminates for the selected cutting conditions.

The maximum developed temperatures reached a steady state inside the hole, which can be interpreted as the highest temperature point of the cutting edge moved from the centre of the hole towards the hole edge, as the drill bit exited the material. The maximum temperatures showed similar values for 50–100 m/min and 150–200 m/min cutting speeds sets. The first set of cutting conditions developed higher maximum temperatures, what can be attributed to the increased cutting times at lower cutting speeds.

All the studied cutting conditions exhibited a significant drop of the maximum temperature developed from the hole edge outward, however the behaviour was different for each cutting speeds set. 150–200 m/min exhibited a higher thermal gradient and concentrated the heat inside the borehole at more than 50–100 m/min cutting speeds set, which presented a smoother transition even from inside the borehole. This behaviour can be explained because lower cutting speeds allowed more time to spread as the drilling
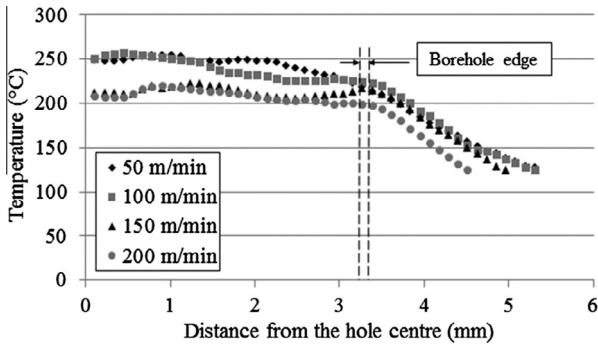
Fig. 7. Maximum temperatures profiles in the drilling of MTM44-1 CF0300 composite corresponding to the considered cutting conditions.

operation was performed, exerting more influence than the decreased thermal conductivity at temperatures above T_g [27]. It was reported in our earlier study that the high strength carbon fibres were more abrasive and produced a brushing effect in contact with the tool due to their lower degree of crystallinity and higher failure strain compared to the high modulus carbon fibres [18]. This can explain the higher maximum temperatures developed by the lower cutting speeds set. This could also explain a more efficient machining process (more energy going into the cutting process rather than being dissipated in the form of heat) at higher cutting speeds, however further investigations in the energetics of CFRP drilling, similar to earlier studies in the drilling of metals [32,33], are required to enable the full explanation of the phenomena developed during the complex drilling process in CFRPs.

Figs. 8–10 show the surface topography of the drilled profiles corresponding to the last drilled hole of each condition at the hole entry, middle and exit zones respectively.

Fig. 8 shows that surface damage at the hole entry increased with the increasing cutting and feed speeds. This difference is especially noticeable between the lowest and the highest cutting conditions, which produced smooth and catastrophically damaged surfaces respectively. However, 1000× magnification images (Fig. 8(e)–(h)) also revealed sub-surface damage, in different extents, for each cutting condition. Sub-surface damage was developed in the areas where the cutting forces were perpendicular to the fibres and where the structural integrity of the composite depended on the mechanical properties of the matrix. 49.8 m/min and 99.6 m/min cutting speeds yielded limited matrix micro-cracking, which increased with the growing cutting speed and produced significant matrix micro-cracking and crack coupling (Fig. 8(g)). The highest cutting speed developed further damage, which resulted in extensive fibre–matrix debonding and surface splintering (Fig. 8(h)).

Similar surface topography features were observed in the middle areas of the inspected holes (Fig. 9). High cutting speeds produced increased matrix cracking, cracking coupling and fibre–matrix debonding. Cracks formed and coupled in a preferential direction, parallel to 90° fibres. This can be explained due to the shear stress produced by the difference in the capacity to bear the load in this direction by 0° and 90° fibres. On the other hand, low cutting speeds yielded significant fibre debonding and pull-out (Fig. 9(e) and (f)) that can be explained by the high temperatures developed at these cutting speeds.

Fig. 10 illustrates the damage in the areas near the hole exit corresponding to the selected cutting conditions. No appreciable damage was observed at the exit of the hole machined at the lowest cutting speed (Fig. 10(a) and (e)). 99.6 m/min cutting speed developed localised matrix cracking at surface levels under the surface hole exit. Localised subsurface cracking was also observed at 149.4 m/min cutting speed, however accompanied by further micro-cracking at surface levels away from the hole exit surface (Fig. 10(c) and (g)). The highest cutting speed yielded visible matrix cracking and significant damage on the hole exit surface, as revealed by the absence of the original hole exit surface (Fig. 10).

In our previous investigations [18], we obtained the material constants (n, C) for MTM44-1 CF0300 composite at the selected feed rate to predict the tool life and tool wear, applying Taylor's model [34]. Therefore, the predicted flank wear extent in drilling 16 holes at 50 m/min, 100 m/min, 150 m/min and 200 m/min cutting speeds and 0.05 mm/rev feed rate are 10.33 μm, 15.66 μm, 17.44 μm and 18.33 μm respectively. These predicted low values of tool wear indicate that the contribution of tool wear on the temperatures developed and machined surface damage can be considered negligible.
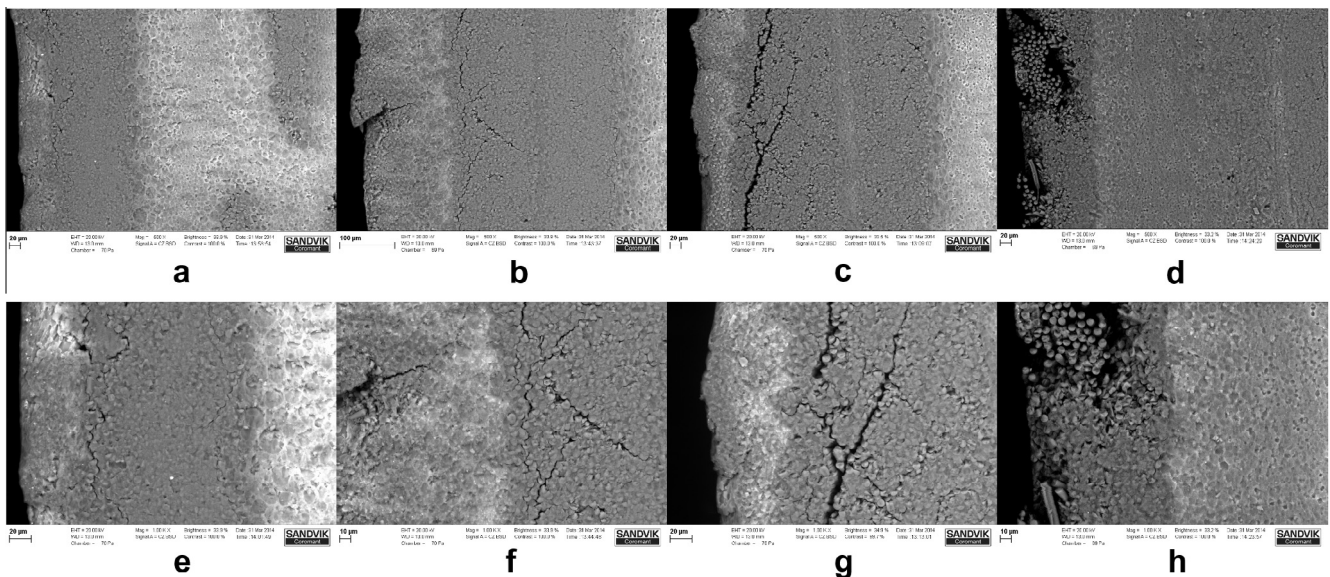

Fig. 8. SEM images at the hole entry corresponding to 49.8 m/min (a, e), 99.6 m/min (b, f), 149.4 m/min (c, g) and 199.2 m/min (d, h) cutting speeds; at 500× (a–d) and 1000× (e–h) magnifications. Machining direction: left to right. The images show fibres in 90° orientation, perpendicular to the machining direction.
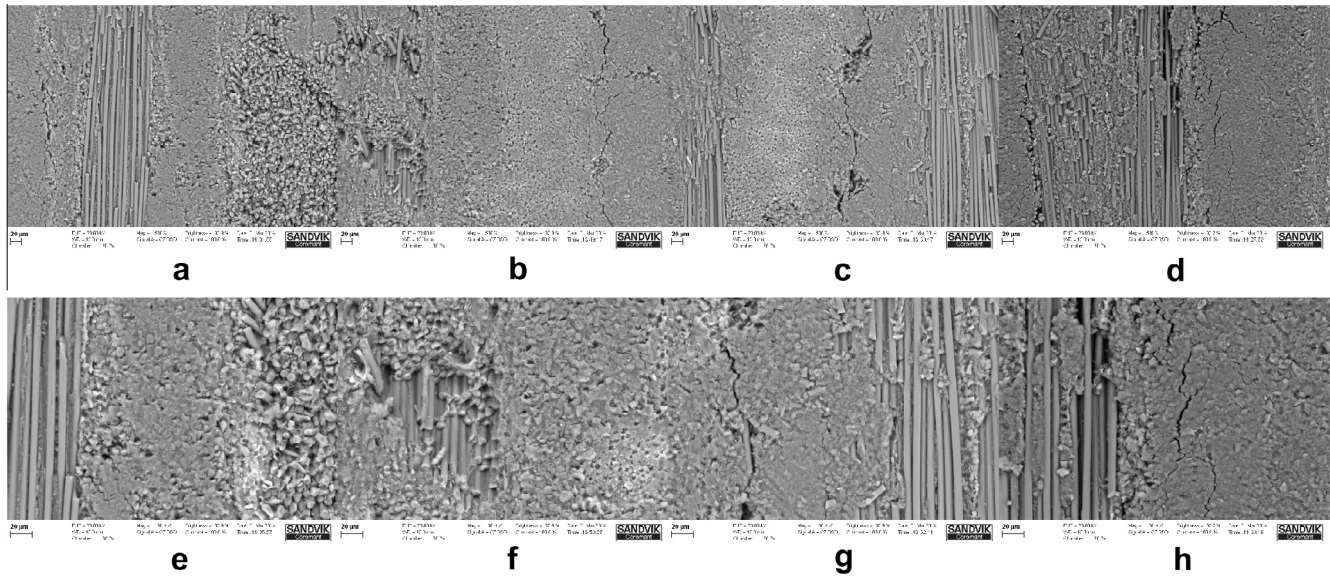
Fig. 9. SEM images of the hole middle areas corresponding to 49.8 m/min (a, e), 99.6 m/min (b, f), 149.4 m/min (c, g) and 199.2 m/min (d, h) cutting speeds; at 500× (a–d) and 1000× (e–h) magnifications. Machining direction: left to right. The images show fibres in 0° and 90° orientations, perpendicular to the machining direction.

Fig. 10. SEM images at the hole exit corresponding to 49.8 m/min (a, e), 99.6 m/min (b, f), 149.4 m/min (c, g) and 199.2 m/min (d, h) cutting speeds; at 500× (a–d) and 1000× (e–h) magnifications. Machining direction: left to right. The images show fibres in 0° and 90° orientations, perpendicular to the machining direction.
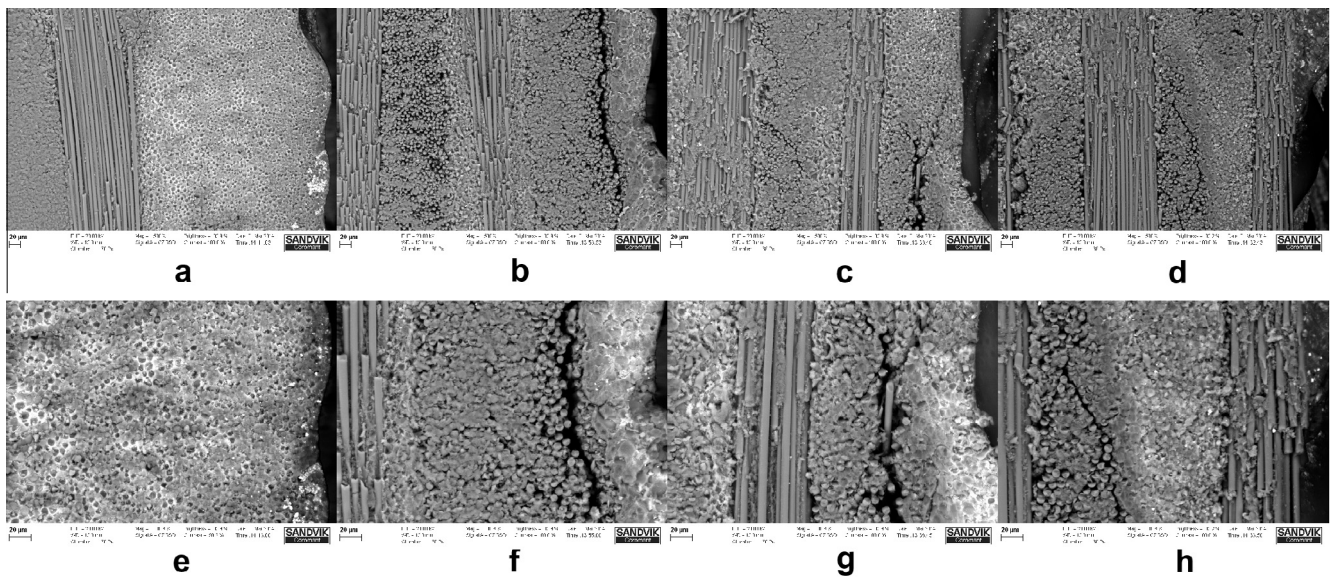
4. Conclusions

This investigation presented the influence of the material properties and the effect of the cutting speed variation on the heat dissipation in the drilling of the studied CFRP composites. Based on the obtained experimental results, the conclusions can be summarised as follows:

- Maximum temperatures developed in the workpiece in CFRP drilling, measured at the hole exit, can be reliably measured using the thermocouples and thermal imaging techniques. Both techniques measured close values of temperatures and thermal gradients during the machining process. However, thermocouples presented some limitations due to their low response times and more complicated set-up compared to the thermal imaging. Therefore, the thermal imaging showed to be a better method for this application.

- The type of polymer matrix showed to have an important influence on the maximum developed temperatures. Resins having higher cross-linking density and closer-packed molecular networks exhibited higher heat dissipation, glass transition temperature and thermal stability compared to those having lower cross-linking density.

- The type of carbon fibre reinforcement exhibited a significant influence on the heat dissipation. CFRP composites having high modulus CF reinforcement yielded lower thermal gradients than those having high strength CF reinforcement. The observed differences in the thermal conductivity of the considered CFRP composites can be explained by the increased crystalline structure and higher orientation parallel to the fibre axis of the high modulus CF, compared to the high strength CF.

- High cutting speeds yielded higher thermal gradients outside the hole edge than low cutting speeds. This suggests that the cutting process would be more efficient in the range of high

cutting speeds, where the cutting energy is used in the cutting process rather than being transformed into heat. However, further investigation of the energetics in CFRP composites drilling is necessary to clarify this point.

- SEM inspection showed that high cutting speeds caused more severe matrix cracking and hole entry/exit splintering than low cutting speeds. However, no damage that suggested matrix burnout or pyrolysis was observed. This indicates that the temperatures developed did not exceed the decomposition temperature of the matrix within the machining time.

Acknowledgements

References

[1] Da Silva MB, Wallbank J. Cutting temperature: prediction and measurement methods – a review. J Mater Process Technol 1999;88(1):195–202.

[2] Davies MA, Ueda T, M'Saoubi R, Mullany B, Cooke AL. On the measurement of temperature in material removal processes. CIRP Ann – Manuf Technol 2007;56(2):581–604.

[3] Ozcelik B, Bagci E. Experimental and numerical studies on the determination of twist drill temperature in dry drilling: a new approach. Mater Des 2006;27(10):920–7.

[4] Weinert K, Kempmann C. Cutting temperatures and their effects on the machining behaviour in drilling reinforced plastic composites. Adv Eng Mater 2004;6(8):684–9 (p. 612).

[5] Le Coz G, Marinescu M, Devillez A, Dudzinski D, Velnom L. Measuring temperature of rotating cutting tools: application to MQL drilling and dry milling of aerospace alloys. Appl Therm Eng 2012;36(1):434–41.

[6] Kerrigan K, Thil J, Hewison R, O'Donnell GE. An Integrated Telemetric Thermocouple Sensor for Process Monitoring of CFRP Milling Operations. Procedia CIRP. vol. 1, 2012. p. 449-54.

[7] Komanduri R, Hou ZB. A review of the experimental techniques for the measurement of heat and temperatures generated in some manufacturing processes and tribology. Tribol Int 2001;34(10):653–82.

[8] Bono M, Ni J. A method for measuring the temperature distribution along the cutting edges of a drill. J Manuf Sci Eng Trans ASME 2002;124(4):921–3.

[9] Yashiro T, Ogawa T, Sasahara H. Temperature measurement of cutting tool and machined surface layer in milling of CFRP. Int J Mach Tools Manuf 2013;70:63–9.

[10] San Juan M, Martín O, Santos FJ, Cabezudo JA, Sánchez A. Study of temperature and workpiece damage in drilling of carbon fiber composites; 2012. p. 495–501.

[11] Tian T, Cole KD. Anisotropic thermal conductivity measurement of carbon-fiber/epoxy composite materials. Int J Heat Mass Transfer 2012;55(23–24):6530–7.

[12] Sato M, Aoki T, Tanaka H, Takeda S. Variation of temperature at the bottom surface of a hole during drilling and its effect on tool wear. Int J Mach Tools Manuf 2013;68:40–7.

[13] Chen WC. Some experimental investigations in the drilling of carbon fiber-reinforced plastic (CFRP) composite laminates. Int J Mach Tools Manuf 1997;37(8):1097–108.

[14] Rawat S, Attia H. Wear mechanisms and tool life management of WC-Co drills during dry high speed drilling of woven carbon fibre composites. Wear 2009;267(5–8):1022–30.

[15] Knibbs RH, Morris JB. The effects of fibre orientation on the physical properties of composites. Composites 1974;5(5):209–18.

[16] Pilling MW, Yates B, Black MA, Tattersall P. The thermal conductivity of carbon fibre-reinforced composites. J Mater Sci 1979;14(6):1326–38.

[17] Trostyanskaya EB, Kobets LP, Gunyaev GM. Investigation of the modulus of elasticity of carbon fibers. Polym Mech 1974;7(5):757–60.

[18] Merino-Pérez JL, Merson E, Ayvar-Soberanis S, Hodzic A. The applicability of Taylor's model to the drilling of CFRP using uncoated WC-Co tools: the influence of cutting speed on tool wear. Int J Mach Mach Mater 2014;16(2):95–112.

[19] Varshney V, Patnaik SS, Roy AK, Farmer BL. A molecular dynamics study of epoxy-based networks: cross-linking procedure and prediction of molecular and material properties. Macromolecules 2008;41(18):6837–42.

[20] Varshney V, Patnaik SS, Roy AK, Farmer BL. Heat transport in epoxy networks: a molecular dynamics study. Polymer 2009;50(14):3378–85.

[21] Yorifuji D, Ando S. Molecular structure dependence of out-of-plane thermal diffusivities in polyimide films: a key parameter for estimating thermal conductivity of polymers. Macromolecules 2010;43(18):7583–93.

[22] Teng CC, Ma CCM, Lu CH, Yang SY, Lee SH, Hsiao MC, et al. Thermal conductivity and structure of non-covalent functionalized graphene/epoxy composites. Carbon 2011;49(15):5107–16.

[23] Lesser AJ, Crawford E. The role of network architecture on the glass transition temperature of epoxy resins. J Appl Polym Sci 1997;66(2):387–95.

[24] Crawford E, Lesser AJ. The effect of network architecture on the thermal and mechanical behavior of epoxy resins. J Polym Sci Part B Polym Phys 1998;36(8):1371–82.

[25] Bandyopadhyay A, Valavala PK, Clancy TC, Wise KE, Odegard GM. Molecular modeling of crosslinked epoxy polymers: the effect of crosslink density on thermomechanical properties. Polymer 2011;52(11):2445–52.

[26] Song F, Zhao H, Hu G. Explicit cross-link relations between effective elastic modulus and thermal conductivity for fiber composites. Comput Mater Sci 2012;51(1):353–9.

[27] Zhong C, Yang Q, Wang W. Correlation and prediction of the thermal conductivity of amorphous polymers. Fluid Phase Equilib 2001;181(1–2):195–202.

[28] Gallego NC, Edie DD. Structure-property relationships for high thermal conductivity carbon fibers. Compos – Part A Appl Sci Manuf 2001;32(8):1031–8.

[29] Yuan G, Li X, Dong Z, Westwood A, Rand B, Cui Z, et al. The structure and properties of ribbon-shaped carbon fibers with high orientation. Carbon 2014;68:426–39.

[30] Banks L, Ellis B. The glass transition temperatures of highly crosslinked networks: cured epoxy resins. Polymer 1982;23(10):1466–72.

[31] Bussu G, Lazzeri A. On the use of dynamic mechanical thermal analysis (DMTA) for measuring glass transition temperature of polymer matrix fibre reinforced composites. J Mater Sci 2006;41(18):6072–6.

[32] Dargnat F, Darnis P, Cahuc O. Energetical approach for semi-analytical drilling modelling. Mach Sci Technol 2008;12(3):295–324.

[33] Dargnat F, Darnis P, Cahuc O. Analytical modelling of cutting phenomena improvements with a view to drilling modelling. Int J Mach Mach Mater 2009;5(2–3):176–206.

[34] Taylor FW. On the art of cutting metals. American Society of Mechanical Engineers; 1907.